Properties of Friction-Stir-Welded 7075 T651 Aluminum

M.W. MAHONEY, C.G. RHODES, J.G. FLINTOFF, R.A. SPURLING, and W.H. BINGEL

Friction stir welding (FSW), a new welding technique invented at TWI, was used to weld 7075 T651 aluminum, an alloy considered essentially unweldable by fusion processes. This weld process exposed the alloy to a short time, high-temperature spike, while introducing extensive localized deformation. Studies were performed on these solid-state welds to determine mechanical properties both in the longitudinal direction, *i.e.*, within the weld nugget, and, more conventionally, transverse to the weld direction. Because of the unique weld procedure, a fully recrystallized fine grain weld nugget was developed. In addition, proximate to the nugget, both a thermomechanically affected zone (TMAZ) and heat affected zone (HAZ) were created. During welding, temperatures remained below the melting point and, as such, no cast or resolidification microstructure was developed. However, within the weld nugget, a banded microstructure that influences room-temperature fracture behavior was created. In the as-welded condition, weld nugget strength decreased, while ductility remained high. A low-temperature aging treatment failed to fully restore T651 strength and significantly reduced tensile ductility. Samples tested transverse to the weld direction failed in the HAZ, where coarsened precipitates caused localized softening. Subsequent low-temperature aging further reduced average strain to failure without affecting strength. Although reductions in strength and ductility were observed, in comparison to other weld processes, FSW offers considerable potential for welding 7075 T651 aluminum.

I. INTRODUCTION

Friction stir welding, a solid-state process invented at TWI (Cambridge, United Kingdom), in 1991, is a viable technique for joining aluminum alloys that are difficult to fusion weld.[1–5] A schematic illustration of the weld process is shown in Figure 1. To friction stir weld either a butt or lap joint, a specially designed cylindrical tool is rotated and plunged into the joint line. The tool has a small diameter entry probe with a concentric larger diameter shoulder. When descended to the part, the rotating entry probe contacts the surface and rapidly friction heats and softens a column of metal. As the probe penetrates beneath the surface, part of this metal column is extruded above the surface. This essentially is the only flash created during the weld process. The depth of penetration is controlled by the tool shoulder and length of entry probe.

When the shoulder contacts the metal surface, its rotation creates additional frictional heat and plasticizes a cylindrical metal column around the inserted pin. During welding, the metals to be joined and the tool are moved relative to each other such that the tool tracks the weld interface. The rotating tool provides a continual hot working action, plasticizing metal within a narrow zone while transporting metal from the leading face of the pin to the trailing edge. Friction stir welding (FSW) is a solid-state joining process with the weld completed without creation of liquid metal.

A moving column of stirred hot metal consumes the weld interface, disrupting and dispersing aluminum surface oxides. The weld cools, not solidifies, as the tool passes, forming a defect-free weld. The process not only generates a heat affected zone (HAZ), but within this HAZ near the weld nugget a thermomechanically affected zone (TMAZ) is also produced, as shown in the micrograph of Figure 2(a) and illustrated schematically in Figure 2(b). Further, as shown in Figure 2(a), the friction stir weld appears broad at the top surface with a smaller well-defined weld nugget in the interior. The weld nugget corresponds to the tool probe that penetrates through the sheet thickness, whereas the broader surface deformation and subsequent surface recrystallization are associated with the rotating tool shoulder. All regions are considered part of the weld microstructure; however, the surface deformation caused by the tool shoulder is relatively shallow in depth.

In a previous article,[6] we reported the influence of the friction stir process on the microstructure of 7075 Al. Being a solid-state process, friction stir welding has the potential to avoid significant changes in microstructure and mechanical properties that usually accompany fusion welds. The objectives of this study were to evaluate changes in tensile properties produced by FSW 7075 T651 Al and to determine the effect, if any, of postweld low-temperature aging.

II. EXPERIMENTAL PROCEDURE

The alloy selected was 6.35-mm gage 7075-T651 Al plate with nominal composition in wt pct 5.6Zn-2.5Mg-1.6Cu-0.23Cr-bal Al that was butt welded using the friction stir technique. All welds were full penetration with the rotating tool probe sufficiently close to the bottom of the plate to include the entire butt joint within the worked and recrystallized microstructure.

Detailed weld parameters, such as tool design and tool rotation speed, are proprietary to TWI's group-sponsored project members. It can be noted, however, that the workpiece travel speed for this study was 12.7 cm/min; the travel speed can be considerably higher, making it comparable in speed to other welding techniques.

M.W. MAHONEY and C.G. RHODES, Senior Scientists, J.G. FLINTOFF and W.H. BINGEL, Members of the Technical Staff, and R.A. SPURLING, Research Scientist, are with the Rockwell Science Center, Thousand Oaks, CA 91360.

Manuscript submitted September 10, 1997.

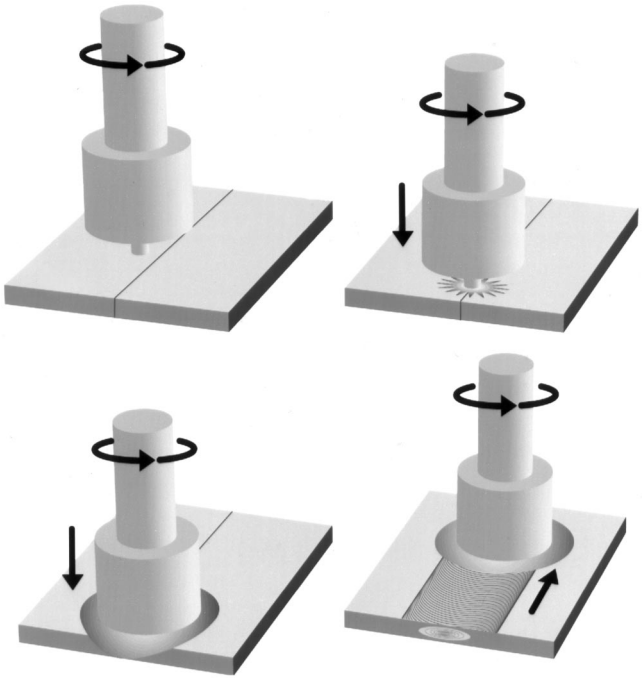

Fig. 1—Schematic illustration of the friction-stir-weld process: (*a*) rotating tool prior to penetration into the butt joint; (*b*) tool probe makes contact with the part, creating heat; (*c*) shoulder makes contact, restricting further penetration while expanding the hot zone; and (*d*) part moves under the tool, creating a friction-stir-weld nugget.

Butt welding 6.35-mm gage plate produced a full penetration weld nugget approximately 10-mm wide. Figure 2(a) shows a low magnification micrograph of the weld nugget, while Figure 2(b) schematically illustrates details of the weld process with resultant details of microstructural features that correspond to Figure 2(a). Unique to the FSW process is the creation of a TMAZ. The TMAZ experiences both temperature and deformation during FSW, as illustrated by the uplifting of grains adjacent to the weld nugget, but insufficient deformation to cause recrystallization. The peak temperatures listed in Figure 2(b) are approximate to the indicated locations with more exacting temperature measurements provided in the text. Temperature measurements were made by imbedding thermocouples proximate to the weld nugget, with peak temperatures recorded as the weld tool passed. Temperatures were monitored both as a function of distance from the weld nugget and through the thickness of the sheet. Measurements within the weld nugget are not possible due to the extensive deformation.

Tensile specimens were machined from the friction stir weld nugget parallel (longitudinal) and normal (transverse) to the weld. Longitudinal tensile bars had a 3-mm diameter and a 20-mm gage section onto which a 13-mm extensometer was fastened. Longitudinal specimens contained only fully recrystallized fine grains from within the weld nugget. Transverse tensile specimens were 160-mm long with a rectangular cross section, 6 × 19 mm, and a 40-mm gage section. Transverse samples contained microstructures from all four zones, *i.e.*, parent metal, HAZ, TMAZ, and weld nugget. Tensile tests were run at room temperature on an Instron testing machine at an initial strain rate of 0.06/min.

Aging treatments following welding were conducted by heating at 121 °C for 24 hours in an air furnace followed by an air cool. This is the standard T651 full strength aging treatment for solution-treated 7075 Al. Although the alloy used in this study started in the T651 condition, the weld and adjacent region experience a short time high-temperature transient during FSW, producing a decreasing temperature gradient outward from the nugget. The temperatures during FSW are sufficiently high and the times at temperature sufficiently long to influence strengthening precipitate morphologies. The local nucleation, growth, and coarsening processes for strengthening precipitates are a function of temperature, which in turn is now a function of distance from the weld nugget. Since there was no solution treatment applied following FSW, there is a postweld gradient in precipitate distribution. As such, the response to the thermal treatment provided here should not be considered as a conventional T651 age. Accordingly, throughout the article, we will refer to this thermal treatment as a postweld age as opposed to the conventional T651 nomenclature.

In addition to total strain, strain distributions along the gage section of transverse tensile test specimens were analyzed by the application of a finely spaced set of parallel lines. Line separations were then measured before and after straining, providing strain distribution for the different microstructures associated with FSW.

Transmission electron microscopy (TEM) was performed using a PHILIPS* CM30 electron microscope operating at 200 kV. Thin foil samples were made by electropolishing in a nitric acid/methanol solution, sometimes followed by ion cleaning. When particles were large enough, identifications were made by energy dispersive spectroscopy and electron diffraction. Scanning electron microscopy (SEM) was performed on either a CamScan or PHILIPS FESEM microscope operating at 20 kV.

*PHILIPS is a trademark of Philips Electronic Instruments Corp., Mahwah, NJ.

III. RESULTS AND DISCUSSION

A. *Longitudinal Orientation*

1. *Tensile tests*

The longitudinally oriented specimens test the weld nugget only. Compared to the base metal, results presented in Table I for as-welded samples show a reduction in yield and ultimate strengths in the weld nugget, while elongation was unaffected. The reduction in preexisting dislocations and the elimination of the very fine hardening precipitates[6] have apparently led to the reduced strength.

One way to recover the lost tensile strength of the weld nugget microstructure would be to administer a postweld aging treatment. Samples were direct aged at 121 °C/24 h, as addition of a solution treatment was assumed to be impractical for many applications of welded components. As shown in Table I, the aging treatment has recovered a large portion of the tensile yield strength in the weld, but at the expense of ductility and ultimate strength. This result indicates that, in the absence of an artificial age, there could also be embrittlement of the weld nugget during long-term natural aging.

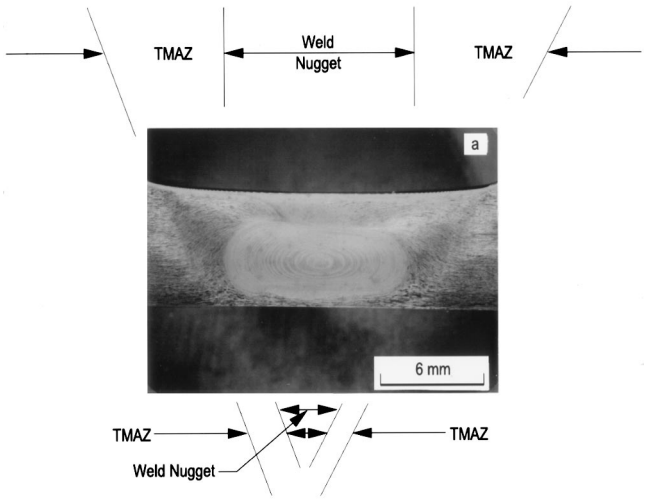

(*a*)

Fig. 2—(*a*) Micrograph of a FSW in 7075 T651 aluminum and (*b*) schematic illustration of friction-stir-weld zone microstructures, precipitate distributions, and temperature ranges for 7075 T651 Al.

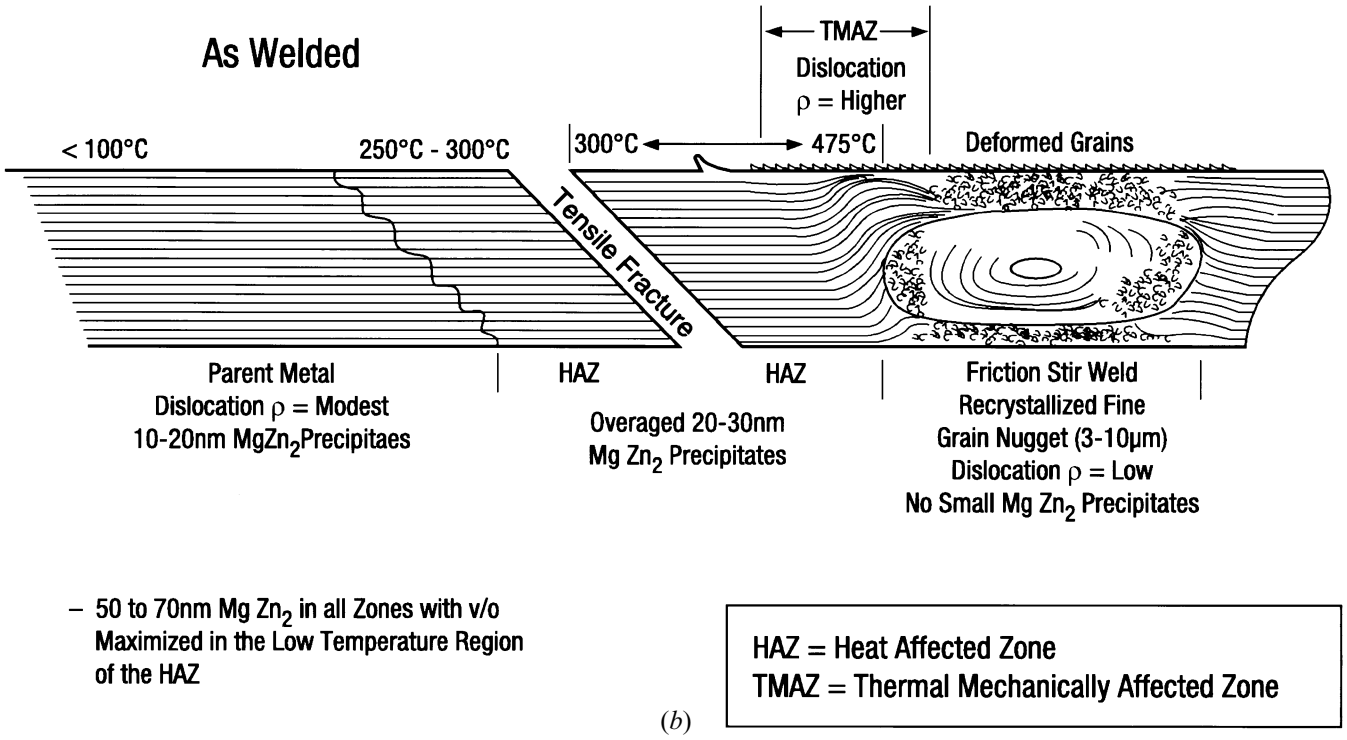

(*b*)

2. *Fractography*

Fractographic examinations of the broken tensile samples from both as-welded and postweld aged conditions reveal roughened fractures containing features having dimensions similar to the grain size of the weld nugget (Figure 3). The more ductile as-welded condition is distinguished by the presence of numerous tear ridges. These ridges reflect the material's ability to sustain the tensile load after microvoid coalescence has begun; absence of the ridges (Figure 3(b)) indicates that the specimen fails soon after microvoid coalescence begins.

The fracture surfaces of both conditions exhibit very fine microvoids on the exposed grain surfaces (Figure 4). These microvoids are smaller in the as-welded condition than those in the postweld aged condition. As will be shown later, at the fracture location, the grains in the postweld aged condition have a precipitate-free zone (PFZ) at the boundaries, whereas the as-welded condition has no PFZs. Ductile grain boundary failure has been studied extensively, and Vasudevan and Doherty have recently summarized the

Table I. Room-Temperature Tensile Properties of Weld Nugget in Friction-Stir-Welded 7075 Al

Condition	Yield Strength (MPa)	Ultimate Strength (MPa)	Elongation (Pct)
Base metal, T651	571	622	14.5
As-friction-stir-welded	365	525	15
Postweld age treatment	455	496	3.5

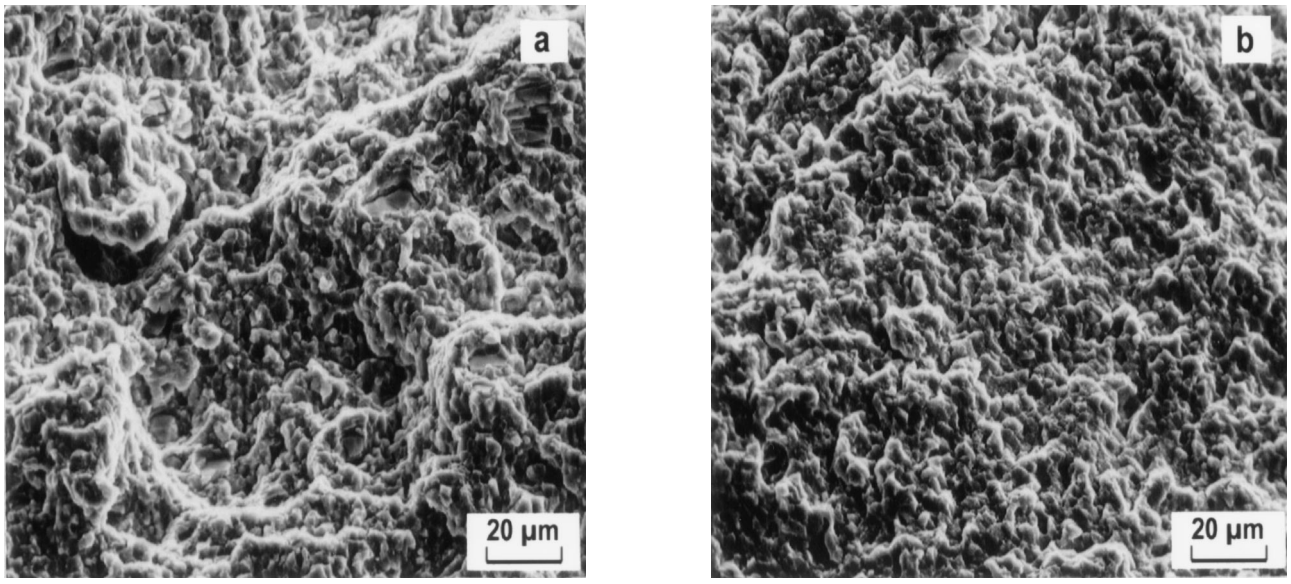

Fig. 3—Intergranular fracture of tensile-tested 7075 Al friction stir welds: (*a*) as-welded and (*b*) postweld aged.

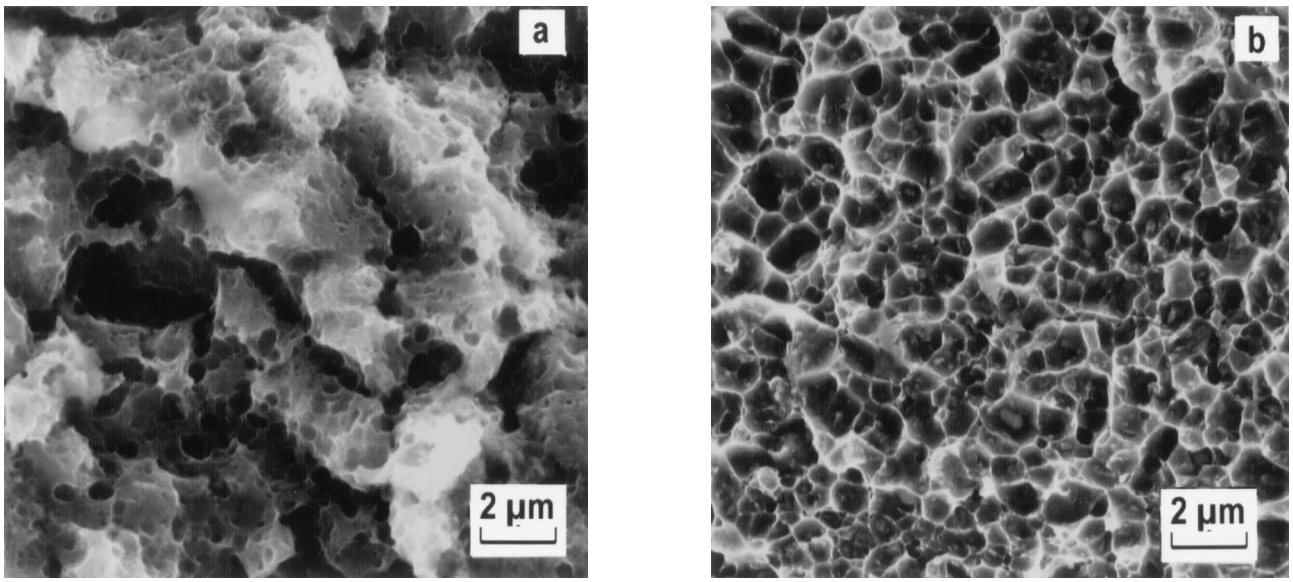

Fig. 4—Fracture surface of FSW sample illustrating fine microvoids on grain surfaces: (*a*) as-welded and (*b*) postweld aged.

phenomenon.[7] They demonstrate that alloys treated to develop PFZs are more ductile than the same alloys in a condition without PFZs. In the present case, then, in the aged condition, the PFZs are more ductile than the grain interiors and fail by microvoid coalescence. In this case, the majority of the strain observed in the tensile test is limited to these very narrow regions of the microstructure. For the as-welded condition, microvoids form at grain boundary particles and coalesce at failure. These two deformation processes have been described by Vasudevan and Doherty,[7] who stated that, ''It may be predicted that an alloy with grain boundary precipitates but no pfz . . . should be . . . more ductile than a similar alloy with a finite pfz.'' This is exactly the behavior observed here, indicating that the presence of PFZs is contributing significantly to the tensile behavior.

Metallographic sectioning through fracture surfaces reveals that the roughened fracture features correspond to individual grains exposed by an intergranular fracture (Figure 5). Profiles of the fractures (Figures 6(a) and 6(b)) suggest that the fracture tends to follow flow lines that develop within the weld nugget for both the as-welded and postaged samples.

3. *Metallography*

The flow lines within the weld nugget are related to the tool design and weld parameters[8] and are characterized by alternating bands of different grain size that we have distinguished, for convenience, as fine (5 to 10 μm) and very fine (3 to 5 μm) recrystallized, equiaxed grains. Backscattered electron imaging of polished surfaces shows that the larger, fine-grain bands have an apparent lower volume

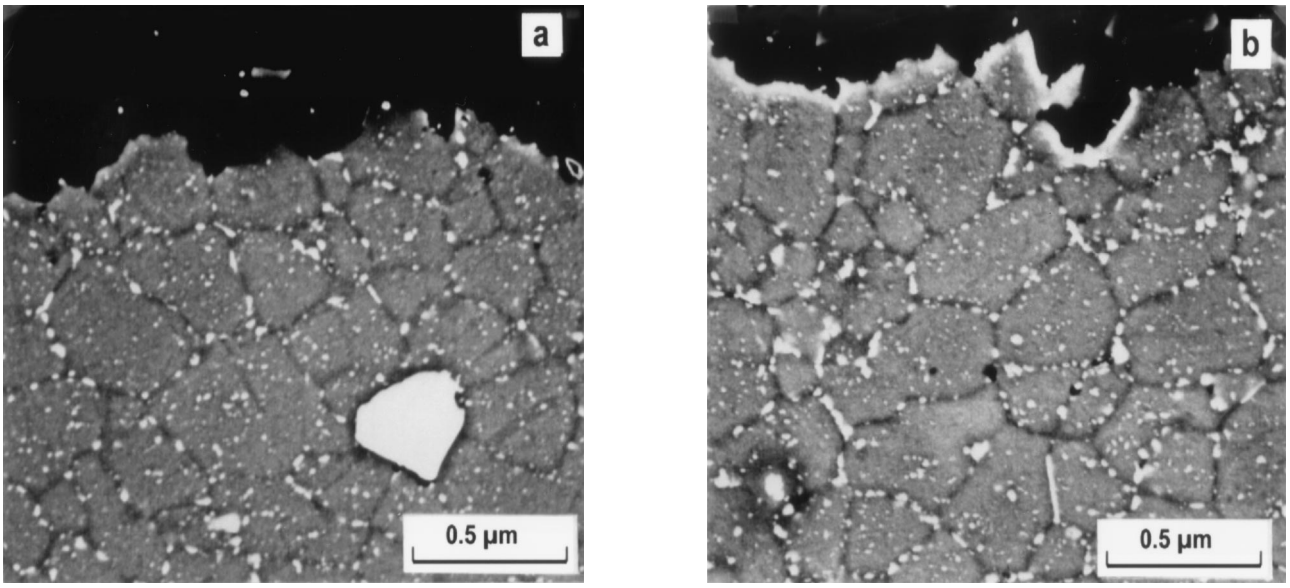

Fig. 5—Cross sections of fracture surfaces shown in Fig. 3. Backscattered electron images of polished surfaces: (*a*) as-welded and (*b*) postweld aged. Note intergranular nature of fractures. Particles include Cr-bearing dispersoids and $MgZn_2$-type precipitates.

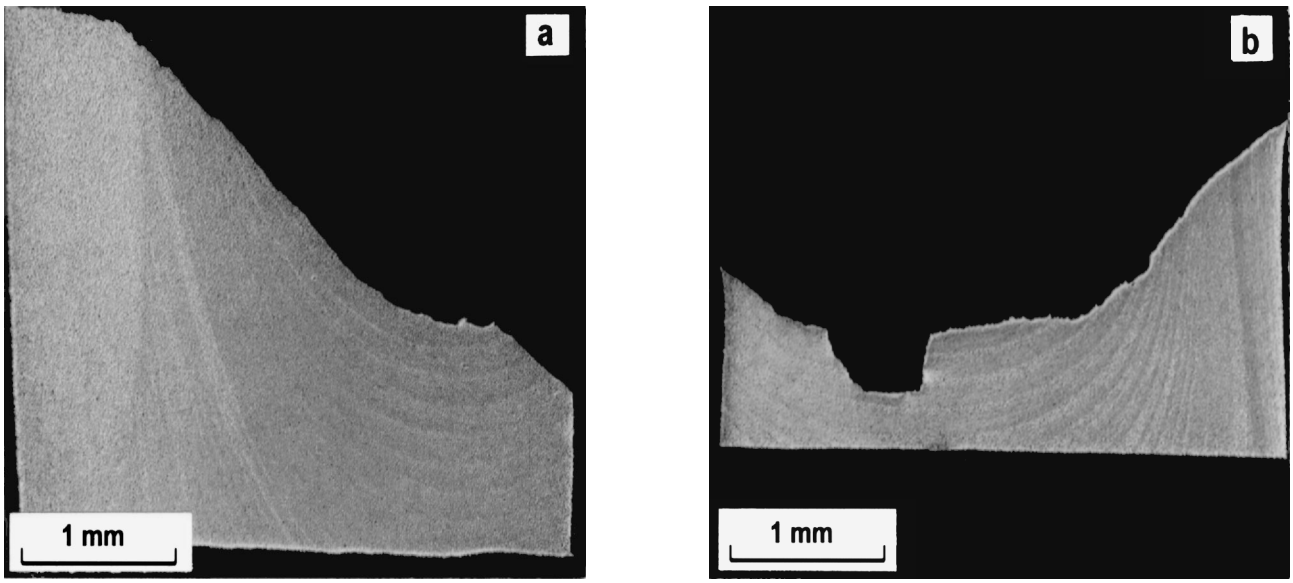

Fig. 6—Metallographic sections through fractured tensile specimens, revealing fracture profiles. (*a*) as welded and (*b*) postweld aged. Note flow line configuration.

fraction of particles, which include Cr-bearing dispersoids and $MgZn_2$-type precipitates, than the smaller, very fine-grain bands (Figure 7). Our work indicates that the banded structure is associated with the threaded tooling.[8,9]

4. *Transmission electron microscopy*

Cross-sectional thin foil results shown in Figures 8 and 9 were taken within ~0.15 mm of the fracture surface. It was clear that both samples, as-welded and welded + aged, were from very fine-grained regions, as the grain size in each was on the order of 3 μm. The as-welded condition contains Cr-bearing dispersoids and $MgZn_2$-type precipitates on the order of 100 nm dispersed relatively uniformly throughout the matrix (Figure 8) and virtually none of the smaller strengthening precipitates.

The aged condition exhibits a duplex population of particles, consisting of dispersoids, ~100 nm, and smaller strengthening precipitates on the order of 5 nm (Figure 9). There is a precipitate-free zone (PFZ), approximately 50- to 100-nm wide, at the grain boundaries.

The total absence of finer precipitates in the as-welded condition leads to the lower yield strength and higher elongation than that in the postweld aged condition. The presence of the 5-nm precipitates in the aged sample contributes to its lower elongation. The PFZ in the latter condition may pro-

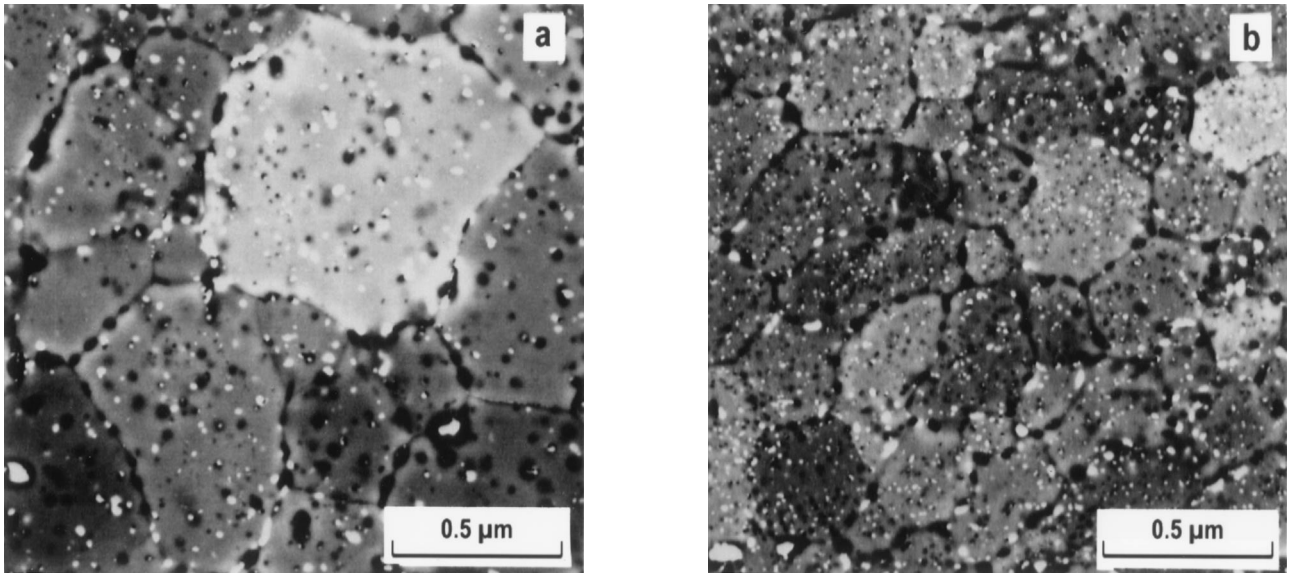

Fig. 7—Backscattered electron images of friction-stir-weld nugget flow lines: (*a*) fine grain size and (*b*) very fine grain size. Note decrease in precipitation in fine grain band (a). Dark particles are Cr-bearing dispersoids and bright particles are $MgZn_2$-type precipitates.

vide a soft fracture zone in the aged sample resulting in the intergranular fracture. The lack of PFZs in the as-welded condition indicates a different mechanism for the intergranular fracture observed in the tensile test. In the as-welded condition, the more ductile grain interiors contribute to the formation of grain boundary voids at hard grain boundary particles. These grain boundary voids then link up at failure, resulting in a ductile intergranular fracture surface.[7]

B. *Transverse Orientation*

1. *Tensile tests*

Compared to unwelded base metal, samples tested transverse to the weld show reductions in strength and elongation (Table II). The as-welded strengths and elongation are also considerably less than those observed for the longitudinal orientation (Table I). In these tests, the region of fracture is not within the weld nugget, as was the case in the longitudinally oriented test specimens, but, as shown later, is within the HAZ. The postweld age treatment did not restore any of the strength to the as-welded condition, and further reduced ductility. Failures in both as-welded and aged conditions were shear fractures in the HAZ.

Figure 10 illustrates the strain distribution across both the weld nugget and HAZs in the as-welded sample. These two regions exhibit differences in strength due to differences in grain size and precipitate size and distribution as a result of exposure to different temperatures for varying times. The higher strength zone, the weld nugget, resists deformation more than the HAZ. This is reflected in the strain results shown in Figure 10, where the lower strength HAZ locally elongated to high levels of strain (12 to 14 pct), eventually resulting in necking and fracture. Conversely, the weld nugget strain (2 to 5 pct) does not reach a failure strain, as considerable additional ductility is available in the weld nugget based on the longitudinal test results. This assumes the equiaxed grain structure results in isotropic behavior (15 pct strain in the weld nugget). The 7.5 pct strain-to-failure reported in Table II is an average strain over the length included within the strain gage, which includes different strength zones. The soft, ductile HAZ in fact corresponds to a short gage length, as reflected in the results shown in Figure 10. Thus, the measure of ductility in transverse tests reflects variations in yield strength of the different HAZs.

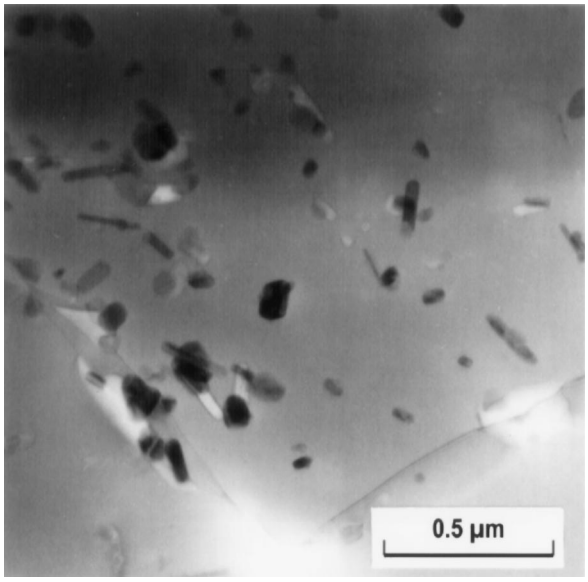

Fig. 8—TEM image of friction-stir-welded 7075 Al showing primarily Cr-bearing dispersoids in the as-welded condition.

In the aged sample, the additional loss in ductility is likely a result of a combination of factors. These include varied aging behavior of precipitates within the different strength zones and a loss of ductility in the weld nugget *via* localization of strain in PFZs.

2. *Fractography*

Fracture surfaces of transverse samples are characterized by long, flat regions, which correspond to the underlying flattened, elongated grains, separated by ductile tear ridges

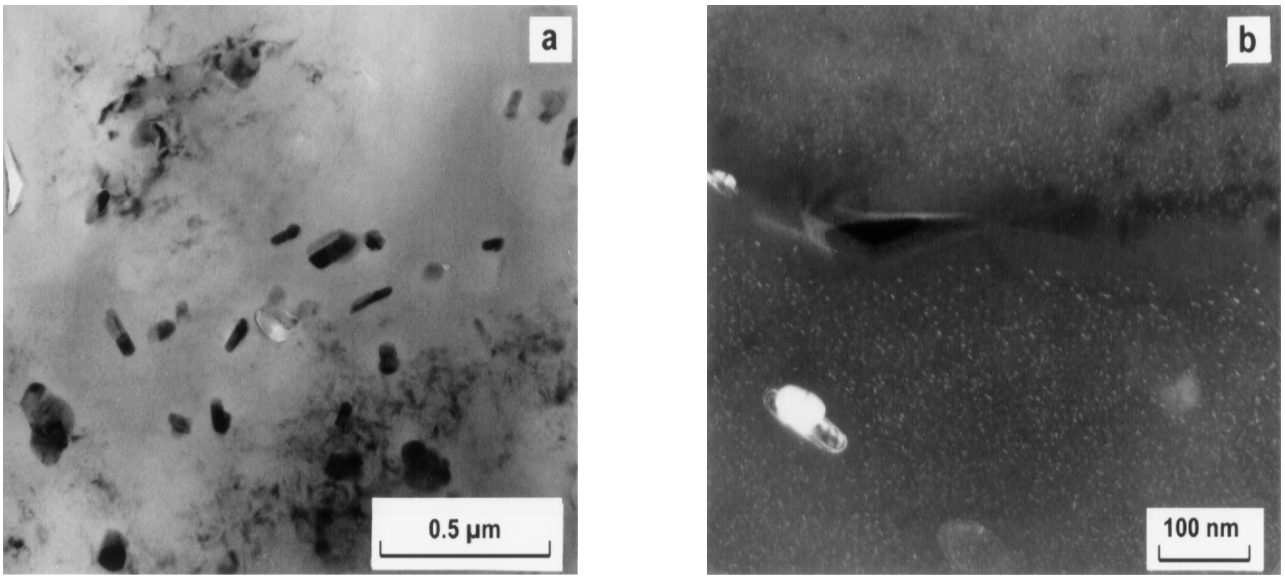

Fig. 9—TEM image of friction-stir-welded 7075 Al showing particles in postweld aged condition: (*a*) dispersoids and $MgZn_2$-type precipitates, bright-field image; and (*b*) smaller precipitates, dark-field image using $MgZn_2$ reflections and presence of grain boundary PFZ.

Table II. Room-Temperature Tensile Properties in Transverse Orientation of Friction-Stir-Welded 7075 Al

Condition	Yield Strength (MPa)	Ultimate Strength (MPa)	Elongation (Pct)
Base metal, T651	571	622	14.5
As-friction-stir-welded	312	468	7.5
Postweld age treatment	312	447	3.5

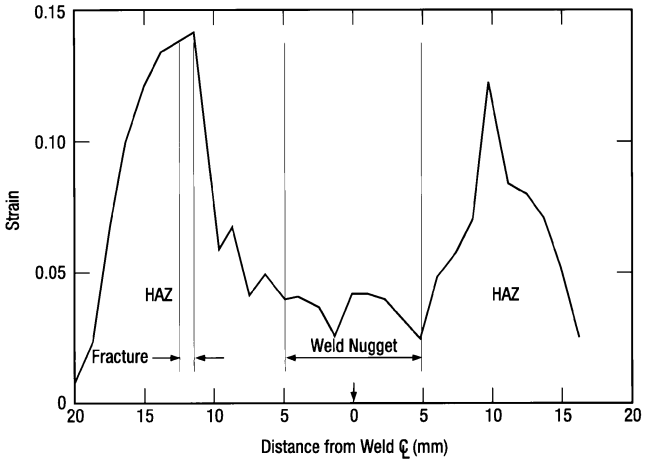

Fig. 10—Tensile strain distribution within the HAZs and weld nugget of a friction stir weld.

(Figure 11). Closer inspection reveals very fine microvoids on the flat surfaces. Although fracture strains are different, there is little difference in fracture appearance between the as-welded and the postweld heat-treated conditions. Apparently, the ductility is sufficient even in the postweld aged condition for a ductile mode of failure.

3. *Metallography*

Failure in both as-welded and thermally aged samples occurs as 45 deg shear fractures (Figure 12). Although shear fractures are typical in rectangular cross-sectional test specimens, in this case, the fracture path also corresponds to the configuration of the temperature profile through the thickness of the sheet.[4] Experimental temperature distribution measurements shown in Figure 13 illustrate that peak temperatures outside the weld nugget vary from 422 °C to 475 °C at the edge of the nugget to 257 °C to 308 °C at a distance of ~11 mm from the nugget. The failures occurred in the lower temperature location of the HAZ, far (~7 to 8 mm measured from the center of the sheet) from the edge of the weld nugget, corresponding to a temperature regime between 300 °C and 350 °C. As shown in Section 4, the fracture site corresponds to a location where strengthening precipitates have coarsened.

4. *Transmission electron microscopy*

Thin foils were taken parallel to, and within ~0.15 mm of, the fracture surfaces. These samples, then, are representative of a plane parallel to the somewhat isothermal contour illustrated in Figure 2(b).

The microstructure of the as-welded condition in the fracture zone exhibits relatively uniformly dispersed strengthening precipitates ($MgZn_2$ type) of roughly two sizes (Figure 14). The larger precipitates are on the order of 30 to 40 nm, and smaller precipitates are about 15 to 30 nm. Also shown in this figure are larger Cr-bearing dispersoids. Both populations of strengthening precipitates are disks ~10 nm in thickness, and their reaction in dark-field imaging suggests these are the same type of precipitate. The particles are dispersed in a matrix consisting of flattened, elongated grains with some of the 30 to 40-nm particles lying in grain boundaries. Occasional larger $MgZn_2$-type (50 to 70 nm) particles are also present.

The postweld aging treatment, 24 hours at 121 °C, has coarsened the strengthening precipitates in the fracture zone, with the larger precipitates being in the range of 50 to 75 nm and smaller ones on the order of 30 nm (Figure 14(b)). (Of course, the dispersoid particles persist after aging.)

These fracture-zone precipitate morphologies differ from

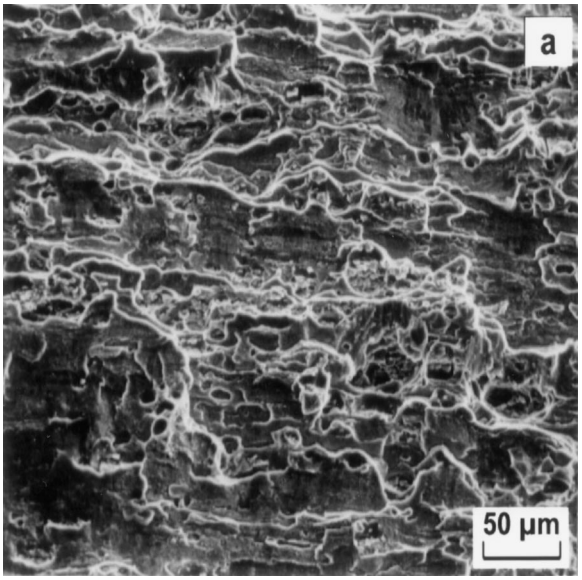

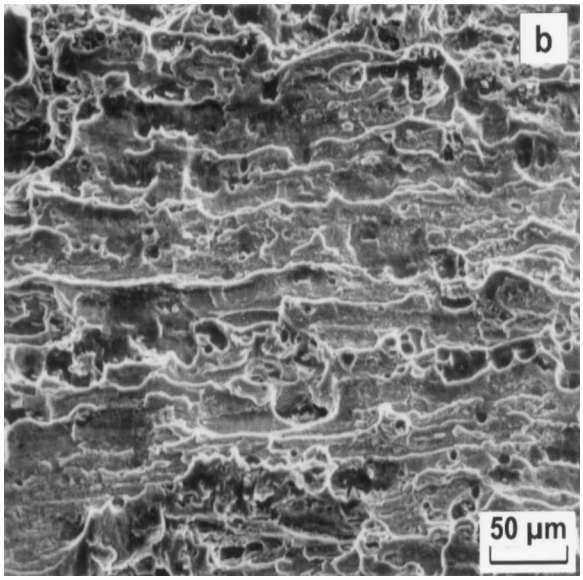

Fig. 11—Fracture surfaces of tensile-tested 7075 Al friction stir welds, transverse orientation: (*a*) as welded and (*b*) postweld aged.

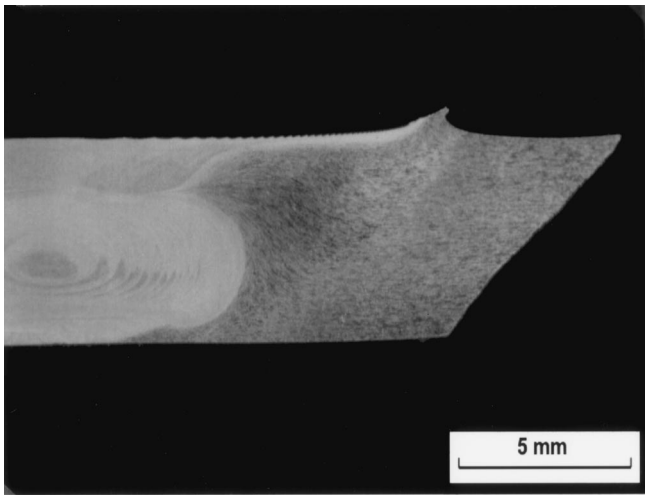

Fig. 12—Cross section of a fracture surface of tensile-tested 7075 Al friction stir weld, transverse orientation, as welded. Postweld age condition showed similar fracture behavior.

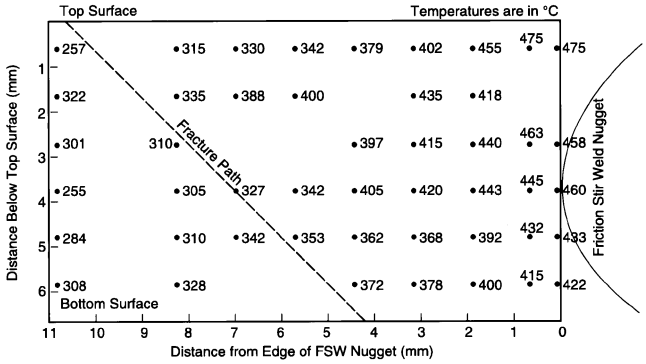

Fig. 13—Peak temperature distribution adjacent to a friction stir weld in 7075 T651 Al.

that of the base metal and that of the hotter region of the HAZ.[6] The base metal contains three populations of precipitates: intergranular ones on the order of 30 to 40 nm, and two sizes of intragranular particles, *viz*. 50 to 75 nm (Cr-bearing dispersoids) and 10 to 15 nm (strengthening precipitates). Compared to the base metal, the fracture zones in both the as-welded and postweld age conditions contain a higher total density of larger particles (dispersoids plus strengthening precipitates) and lower density of very fine particles, which will contribute to the lower yield strength in the fracture zone. A summary of the particle distributions is given in Table III. (Because thicknesses of TEM thin foils cannot easily be accurately measured, statistically correct particle distributions and volume fractions have not been made. The particle sizes were measured and the ''volume fractions'' reported in Table III were qualitatively estimated from TEM observations. From these observations, however, relative volume fractions can be made with a high degree of reliability.)

The hotter region of the HAZ (that between the fracture zone and the weld nugget) contains none of the 10- to 15-nm particles, but has a higher volume fraction of the larger, 50- to 100-nm particles. These larger particles include both the Cr-bearing dispersoids and the $MgZn_2$-type precipitates (Table III), with the added $MgZn_2$ precipitates accounting for the increase in volume fraction. Yet this region, with none of the smaller strengthening precipitates, has a higher flow stress than the fracture zone, which has a distribution of smaller strengthening precipitates (Figure 10). One explanation for this observed behavior is that the larger strengthening precipitates contribute significantly to the strength of this alloy.

These different regions of the HAZ, their precipitate distributions, and approximate temperatures during welding are schematically illustrated in Figure 2(b). The temperature gradient that develops during the welding process produces a gradient of microstructures from the center of the weld nugget to unaffected base metal. Strain measurements presented in Figure 10 show that the fracture zone corresponds to the region in the HAZ that is least resistant to strain, *i.e.*, has a lower flow stress, indicating this zone has been stressed well beyond its yield strength. The TEM studies across the weld zone from nugget to base metal show that

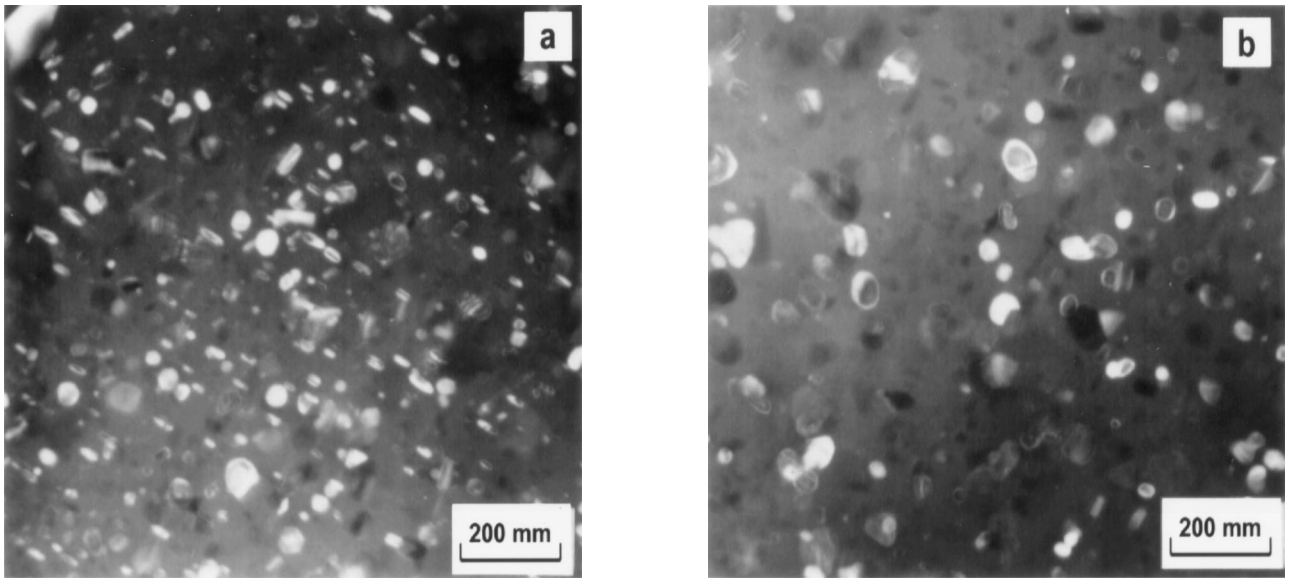

Fig. 14—Dark-field TEM images of friction-stir-welded 7075 Al showing precipitates in fracture zone using $MgZn_2$ reflection: (*a*) as-welded transverse specimen and (*b*) postweld aged transverse specimen.

Table III. Summary of Particle Distributions (As-Welded Condition)

Particle Type	Parent Metal	Fracture Zone	Hotter HAZ	Weld Nugget
50 to 100-nm Cr-bearing dispersoids	yes	yes	yes	yes
50 to 70-nm $MgZn_2$-type precipitates	no	few	yes	rare
30 to 40-nm $MgZn_2$-type precipitates	yes	yes	rare	no
5 to 15-nm strengthening precipitates	yes	no	no	no
15 to 30-nm strengthening precipitates	no	yes	no	no

there are no fine (10 to 15 nm) precipitates in the HAZ between the tensile fracture zone and the nugget, while there is a decreasing volume fraction of the larger (75 to 100 nm) strengthening precipitates (the dispersoid population remains fairly constant). This particle distribution is the result of the maximum temperature reached during the welding process: fine particles are completely dissolved and larger particles are partially dissolved above 350 °C. There is then some growth of the larger particles during cooling.

The fracture zone in the as-welded condition exhibits coarsened fine precipitates, suggesting an overaged condition which will not be as strong as the base metal. The weld nugget region, even with all strengthening precipitates in solution, is also stronger than the HAZ (Table I), forcing the fracture into the HAZ.

It is not obvious from the microstructure why the postweld aged condition should exhibit lower ductility than the as-welded condition. Perhaps the answer lies in the extent of the increased difference in strengths between the weaker (fracture zone) region and the surrounding regions. That is, if the aging treatment has further strengthened the nugget and near-nugget zones, the yield strength of the surrounding region may never be reached before the weaker fracture zone region fails. Thus, total elongation of the tensile sample will be limited to the fracture zone and be measured as a lower extension than that in the as-welded condition in which yielding in the surrounding material contributes to the total elongation.

IV. CONCLUDING REMARKS

Longitudinal and transverse (to the weld) tensile testing has demonstrated that the weakest region associated with FSW is the lower temperature location within the HAZ zone about 7 to 8 mm from the edge of the weld nugget. The yield strength of this location is about 45 pct less than that of the base metal, while the ultimate strength is about 25 pct less. In weldable Al alloys, typically, the weld zone exhibits a 30 to 60 pct reduction in yield and ultimate strengths,[10,11] so the losses due to the friction stir process are at the lower end of the range for Al alloys.

A. *Weld Nugget Properties*

There was a 35 pct loss of yield strength and 15 pct loss of ultimate strength, and no loss of ductility, within the weld nugget, when compared to the base metal. Although this strength loss is significant, it is far less than the loss generally encountered with a fusion weld of weldable aluminum alloys.[10] The loss of yield and ultimate tensile strengths within the weld nugget can be linked to the change in microstructure. The previous study[6] demonstrated, and this work confirms, a reduction in fine hardening precipitate particles and dislocations within the weld nugget, which will contribute to a lower strength.

Postweld thermal aging was aimed at restoring the tensile strength without administering a solution treatment, as a postweld solution treatment is not practical for many applications of aluminum alloy welds. Although the aging treatment recovered a significant portion of the lost strength, there was an accompanying loss in ductility. The increase in the volume fraction of fine hardening precipitates has apparently led to the improved strength and the

loss of ductility. In addition, the intergranular nature of the fracture suggests that the PFZs at grain boundaries are the weak link in the microstructure.

The flow lines attributable to the friction stir weld tool design clearly influence the fracture path of the weld nugget. The differences in grain size and precipitate distribution may account for the location and direction of the fracture path.

B. *Transverse Properties*

Fracturing in a shear mode well away from the weld nugget suggests a softening due to thermal effects, *i.e.*, in a HAZ. Heating characteristics of the workpiece during the welding process result in a wider hot zone at the top surface (due to tool shoulder friction heating) and a narrower zone at the bottom surface (due to heat extraction by the base plate). Isothermal contours in the cross section of the weld zone will thus angle from the top surface toward the nugget as they approach the bottom surface. The fracture path in the tensile samples follows such a contour. The particular contour along which the fracture occurs has reached 300 °C to 350 °C, a regime where larger strengthening precipitates coarsen at the expense of the fine ones, resulting in an overaged condition.

Postweld thermal aging had no effect on yield strength and lowered ultimate strength and elongation. The fracture contour was ~2 mm closer to the nugget when compared to the as-welded condition, indicating an even weaker zone at this position. One possible explanation is the increased strengthening of the surrounding regions due to the aging treatment.

ACKNOWLEDGMENTS

We are pleased to acknowledge the experimental assistance of Michael Calabrese and April Beaudine. We are also grateful to Dr. D.A. Hardwick, Science Center, and Professor J.A. Wert, University of Virginia, for constructive reading of the manuscript.

REFERENCES

1. W.M. Thomas, E.D. Nicholas, J.C. Needham, M.G. Murch, P. Templesmith, and C.J. Dawes: ''Friction Stir Butt Welding,'' International Patent Application No. PCT/GB92/02203 and GB Patent Application No. 9125978.8, Dec. 1991, U.S. Patent No. 5,460,317, Oct. 1995.
2. C.J. Dawes and W.M. Thomas: *TWI Bull. 6*, 1995, vol. 124.
3. M. Ellis and M. Strangwood: *TWI Bull. 6*, 1995, vol. 138.
4. C.J. Dawes and W.M. Thomas: *Weld. J.* 1996, vol. 75 (3), p. 41.
5. O.T. Midling: *Proc. 4th Int. Conf. on Aluminum Alloys*, Atlanta, GA, Sept. 1994.
6. C.G. Rhodes, M.W. Mahoney, W.H. Bingel, R.A. Spurling, and C.C. Bampton: *Scripta Metall.*, 1997, vol. 36, pp. 69-75.
7. A.K. Vasudevan and R.D. Doherty: *Acta Metall.*, 1987, vol. 35, pp. 1193-1219.
8. M.W. Mahoney: Rockwell Science Center, Thousand Oaks, CA, unpublished research, 1997.
9. *Weld. Met. Fabr.*, 1995, June, p. 214.
10. *Metals Handbook*, 9th ed., ASM, Metals Park, OH, 1983, vol. 6, p. 373.
11. *ASM Handbook*, 1st ed., ASM, Materials Park, OH, 1993, vol. 6, p. 729.